

## Elucidation of the Mechanism in Fluorine-Free Prepared $\text{YBa}_2\text{Cu}_3\text{O}_{7-\delta}$ Coatings

Pieter Vermeir,<sup>\*,†,‡</sup> Iwein Cardinael,<sup>§</sup> Joseph Schaubroeck,<sup>†</sup> Kim Verbeken,<sup>§</sup> Michael Bäcker,<sup>||</sup> Petra Lommens,<sup>‡</sup> Werner Knaepen,<sup>⊥</sup> Jan D'haen,<sup>⊗</sup> Klaartje De Buysser,<sup>‡</sup> and Isabel Van Driessche<sup>‡</sup>

<sup>†</sup>Faculty of Applied Engineering Sciences, University College Ghent, Schoonmeersstraat 52 (C), 9000 Ghent, Belgium, <sup>‡</sup>Department of Inorganic and Physical Chemistry, Ghent University, Krijgslaan 281 (S3), 9000 Ghent, Belgium, <sup>§</sup>Department of Materials Science and Engineering, Ghent University, Technologiepark 903, 9052 Zwijnaarde, Belgium, <sup>||</sup>Zenergy Power GmbH, Heisenbergstrasse 16, 53359 Rheinbach, Germany, <sup>⊥</sup>Department of Solid State Sciences, Ghent University, Krijgslaan 281 (S1), 9000 Ghent, Belgium, and <sup>⊗</sup>Imec, Division Imomec, Wetenschapspark 1, 3590 Diepenbeek, Belgium

Received November 4, 2009

In this work, the reaction mechanism used in the preparation of fluorine-free superconducting  $\text{YBa}_2\text{Cu}_3\text{O}_{7-\delta}$  (YBCO) was investigated. To determine which precursor interactions are dominant, a comprehensive thermal analysis (thermogravimetric analysis-differential thermal analysis) study was performed. The results suggest that a three step reaction mechanism, with a predominant role for  $\text{BaCO}_3$ , is responsible for the conversion of the initial state to the superconducting phase. In the presence of  $\text{CuO}$ , the decarboxylation of  $\text{BaCO}_3$  is kinetically favored with the formation of  $\text{BaCuO}_2$  as a result.  $\text{BaCuO}_2$  reacts with the remaining  $\text{CuO}$  to form a liquid which ultimately reacts with  $\text{Y}_2\text{O}_3$  in a last step to form YBCO. High temperature X-ray diffraction experiments confirm that these results are applicable for thin film synthesis prepared from an aqueous fluorine-free sol–gel precursor.

### Introduction

The development of low-cost deposition techniques for high performance  $\text{YBa}_2\text{Cu}_3\text{O}_{7-\delta}$  (YBCO) coated conductors is one of the major objectives in obtaining a widespread use of superconductivity in power applications.<sup>1–3</sup>

During the past decade, various processing techniques were successfully applied to prepare high critical current YBCO thin films.<sup>4–6</sup> Non-vacuum techniques, overall classified as Chemical Solution Deposition (CSD) routes, are preferred over vacuum techniques because they show favorable features including (i) lower investments, (ii) faster

deposition rates with higher yields, and most importantly (iii) processing under ambient pressure enabling a continuous process.<sup>7</sup>

Among the different precursor designs described for the synthesis of YBCO coated conductors using CSD,<sup>8–16</sup>

\*To whom correspondence should be addressed. E-mail: pieter.vermeir@ugent.be. Fax: +3292644983. Phone: +3292644550.

(1) Holesinger, T. G.; Civale, L.; Maiorov, B.; Feldmann, D. M.; Coulter, J. Y.; Miller, J.; Maroni, V. A.; Chen, Z. J.; Larbalestier, D. C.; Feenstra, R.; Li, X. P.; Huang, M. B.; Kodenkandath, T.; Zhang, W.; Rupich, M. W.; Malozemoff, A. P. *Adv. Mater.* **2008**, *20*, 391.

(2) Schoofs, B.; Cloet, V.; Vermeir, P.; Schaubroeck, J.; Hoste, S.; Van Driessche, I. *Supercond. Sci. Technol.* **2006**, *19*, 1178.

(3) Zhang, W.; Rupich, M. W.; Schoop, U.; Verebelyi, D. T.; Thieme, C. L. H.; Li, X.; Kodenkandath, T.; Huang, Y.; Siegal, E.; Buczek, D.; Carter, W.; Nguyen, N.; Schreiber, J.; Prasova, M.; Lynch, J.; Tucker, D.; Fleshler, S. *Phys. C (Amsterdam, Neth.)* **2007**, *463*, 505.

(4) Bhuiyan, M. S.; Paranthaman, M.; Salama, K. *Supercond. Sci. Technol.* **2006**, *19*, R1.

(5) Kashima, N.; Niwa, T.; Mori, M.; Nagaya, S.; Muroga, T.; Miyata, S.; Watanabe, T.; Yamada, Y.; Izumi, T.; Shiohara, Y. *Appl. Supercond. Conf.* **2004**, 2763.

(6) Ibi, A.; Iwai, H.; Takahashi, K.; Muroga, T.; Miyata, S.; Watanabe, T.; Yamada, Y.; Shiohara, Y. *Phys. C* **2005**, *426*, 910.

(7) Foltyn, S. R.; Civale, L.; Macmanus-Driscoll, J. L.; Jia, Q. X.; Maiorov, B.; Wang, H.; Maley, M. *Nat. Mater.* **2007**, *6*, 631.

(8) Risse, G.; Schlobach, B.; Hassler, W.; Stephan, D.; Fahr, T.; Fischer, K. *J. Eur. Ceram. Soc.* **1999**, *19*, 125.

(9) Xu, Y.; Goyal, A.; Rutter, N. A.; Shi, D.; Paranthaman, M.; Sathyamurthy, S.; Martin, P. M.; Kroeger, D. M. *J. Mater. Res.* **2003**, *18*, 677.

(10) Rice, C. E.; Vandover, R. B.; Fisanick, G. J. *Appl. Phys. Lett.* **1987**, *51*, 1842.

(11) Hamdi, A. H.; Mantese, J. V.; Micheli, A. L.; Laugal, R. C. O.; Dungan, D. F.; Zhang, Z. H.; Padmanabhan, K. R. *Appl. Phys. Lett.* **1987**, *51*, 2152.

(12) Gross, M. E.; Hong, M.; Liou, S. H.; Gallagher, P. K.; Kwo, J. *Appl. Phys. Lett.* **1988**, *52*, 160.

(13) Falter, M.; Hassler, W.; Schlobach, B.; Holzapfel, B. *Phys. C (Amsterdam, Neth.)* **2002**, *372*, 46.

(14) Manabe, T.; Sohma, M.; Yamaguchi, I.; Tsukada, K.; Kondo, W.; Kamiya, K.; Tsuchiya, T.; Mizuta, S.; Kumagai, T. *Phys. C (Amsterdam, Neth.)* **2006**, *445*, 823.

(15) Obradors, X.; Puig, T.; Pomar, A.; Sandiumenge, F.; Mestres, N.; Coll, M.; Cavallaro, A.; Roma, N.; Gazquez, J.; Gonzalez, J. C.; Castano, O.; Gutierrez, J.; Palau, A.; Zalamova, K.; Morlens, S.; Hassini, A.; Gibert, M.; Ricart, S.; Moreto, J. M.; Pinol, S.; Isfort, D.; Bock, J. *Supercond. Sci. Technol.* **2006**, *19*, S13.

(16) Li, X.; Rupich, M. W.; Kodenkandath, T.; Huang, Y.; Zhang, W.; Siegal, E.; Verebelyi, D. T.; Schoop, U.; Nguyen, N.; Thieme, C.; Chen, Z.; Feldman, D. M.; Larbalestier, D. C.; Holesinger, T. G.; Civale, L.; Jia, Q. X.; Maroni, V.; Rane, M. V. *IEEE Trans. Appl. Supercond.* **2007**, *17*, 3553.

metalorganic deposition using trifluoroacetates (TFA) is the most widespread. This originates from the fact that TFA solutions decompose to carbonate-free precursor films while in fluorine-free CSD processes, the organic precursors lead to the formation of  $\text{BaCO}_3$ . Until recently, it was generally accepted that the presence of this  $\text{BaCO}_3$  kinetically hinders the formation of the YBCO phase, leading to superconducting films of poor quality.<sup>17,18</sup>

Nevertheless, several papers report on the successful preparation of high critical current superconducting films from fluorine-free CSD precursors.<sup>19–23</sup> While most of these methods use organic solvents, we reported in a previous paper the synthesis of YBCO coatings starting from an aqueous solution.<sup>24</sup> In this work, we present a study of (i) the reaction mechanism responsible for the formation of YBCO from fluorine-free CSD precursors and (ii) the role of  $\text{BaCO}_3$  in this.

## Experimental Section

**Precursor Preparation.** Precursor solutions for thin film deposition were fabricated from readily available Y-, Ba-, and Cu-acetates (Sigma-Aldrich). These powders are dissolved in an acetic acid/water mixture (ratio 1:4) to a total metal-ion concentration of 0.6 M. After refluxing at 90 °C for 1 h, triethanolamine (> 99%, Sigma-Aldrich) is added under continuous stirring until a Cu to ligand concentration of 1:5 is obtained. Finally, ammonia (25 wt %, Sigma-Aldrich) is added to adjust the pH between 5 and 7. The complexity to stabilize metal-ions in a water-based environment is described in a previous paper.<sup>25</sup>

For TGA-DTA (Thermogravimetric Analysis-Differential Thermal Analysis) powders of  $\text{Y}_2\text{O}_3$ ,  $\text{BaCO}_3$ , and CuO (Sigma Aldrich) were used. The YBCO sample, supplied by Zenergy Power GmbH, was produced using the melt-grown technique. Small impurities of  $\text{Y}_2\text{BaCuO}_5$  and CuO were detected using XRD (X-ray Diffraction).

**Characterization Techniques.** The thermal decomposition behavior of the various powders was investigated using a TGA-DTA setup from Stanton-Redcroft STA 1500. All powders were ball-milled for 12 h to ensure a homogeneous mixture of small grains. Powders of different metal combinations were mixed in a metal-ratio referring to the stoichiometry in  $\text{YBa}_2\text{Cu}_3\text{O}_{7-\delta}$ .

Micrograph images were taken with a normal light microscope.

HT-XRD (High Temperature X-ray Diffraction) measurements of the  $\text{BaCO}_3$ -CuO and  $\text{Y}_2\text{O}_3$ - $\text{BaCO}_3$ -CuO films were performed using a Bruker D8 Discover. Using a parallel beam geometry in a  $\theta$ - $2\theta$  position, counts were registered with (i) a linear Vantec detector for  $\text{BaCO}_3$ -CuO films and (ii) a position sensitive Si(Li) detector for  $\text{Y}_2\text{O}_3$ - $\text{BaCO}_3$ -CuO films.

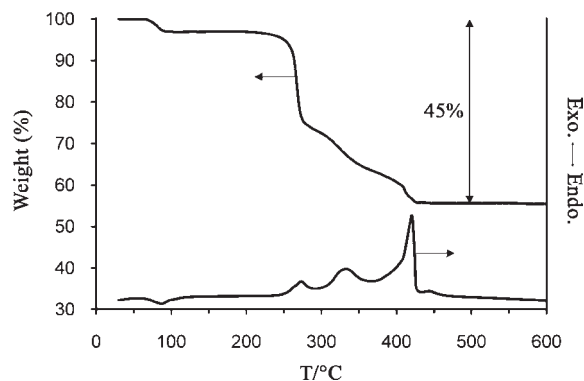


**Figure 1.** TGA-DTA spectrum in air for a mixture containing  $\text{Y}(\text{OAc})_3$ ,  $\text{Ba}(\text{OAc})_2$ , and  $\text{Cu}(\text{OAc})_2$  (Y/Ba/Cu = 1:2:3) heated at  $10\text{ °C min}^{-1}$ .

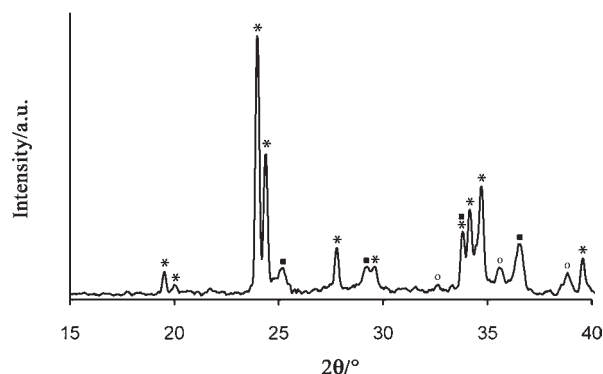


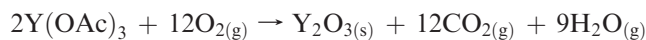
**Figure 2.** XRD spectrum of a mixture containing  $\text{Y}(\text{OAc})_3$ ,  $\text{Ba}(\text{OAc})_2$ , and  $\text{Cu}(\text{OAc})_2$  combusted at 450 °C in air for 24 h (■)  $\text{Y}_2\text{O}_3$  (\*)  $\text{BaCO}_3$  and (○) CuO.

## Results and Discussion

**Part A: TGA-DTA Study.** Fluorine-free CSD precursor solutions all consist of metal-salts that are stabilized in water and/or other solvents.<sup>19–24</sup> Upon transformation of the precursor state to the actual superconducting phase, the respective metal-salts are combusted to  $\text{Y}_2\text{O}_3$ ,  $\text{BaCO}_3$ , and CuO. Depending on the type of precursor and the atmosphere, combustion normally takes place below 500 °C.

As our precursor solutions are prepared from metal-acetates, a TGA-DTA spectrum (Figure 1) was recorded for a powder mixture of  $\text{Y}(\text{OAc})_3 \cdot 2.3\text{H}_2\text{O}$ ,  $\text{Ba}(\text{OAc})_2$ , and  $\text{Cu}(\text{OAc})_2$  in a Y/Ba/Cu ratio of 1:2:3.

After heating this metal-acetate mixture to 440 °C, an experimental mass loss of 45% of the total weight is found. This corresponds well to the theoretical value of 45.2% that can be calculated for the combustion reaction that transforms the respective metal-salts into  $\text{Y}_2\text{O}_3$ ,  $\text{BaCO}_3$ , and CuO, as given below.



XRD analysis of the powder mixture combusted at 450 °C in air for 24 h, as shown in Figure 2, confirms the presence of  $\text{Y}_2\text{O}_3$ ,  $\text{BaCO}_3$ , and CuO.

(17) Parmigiani, F.; Chiarello, G.; Ripamonti, N.; Goretzki, H.; Roll, U. *Phys. Rev. B* **1987**, *36*, 7148.

(18) Hirano, S.; Hayashi, T.; Miura, M. *J. Am. Ceram. Soc.* **1990**, *73*, 885.

(19) Kim, B. J.; Yi, K. Y.; Kim, H. J.; Ahn, J. H.; Kim, J. G.; Hong, S. K.; Hong, G. W.; Lee, H. G. *Supercond. Sci. Technol.* **2007**, *20*, 428.

(20) Long, N.; Campbell, L.; Kemmitt, T.; Kennedy, V. J.; Markwitz, A.; Bubendorfer, A. *J. Electroceram.* **2004**, *13*, 361.

(21) Patta, Y. R.; Wesolowski, D. E.; Cima, M. J. *Phys. C (Amsterdam, Neth.)* **2009**, *469*, 129.

(22) Tsukada, K.; Yamaguchi, I.; Sohma, M.; Kondo, W.; Kamiya, K.; Kumagai, T.; Manabe, T. *Phys. C (Amsterdam, Neth.)* **2007**, *458*, 29.

(23) Xu, Y.; Goyal, A.; Leonard, K.; Martin, P. *Phys. C (Amsterdam, Neth.)* **2005**, *421*, 67.

(24) Vermeir, P.; Cardinael, I.; Backer, M.; Schaubroeck, J.; Schacht, E.; Hoste, S.; Van Driessche, I. *Supercond. Sci. Technol.* **2009**, *22*, 075009.

(25) Schoofs, B.; Van de Vyver, D.; Vermeir, P.; Schaubroeck, J.; Hoste, S.; Herman, G.; Van Driessche, I. *J. Mater. Chem.* **2007**, *17*, 1714.

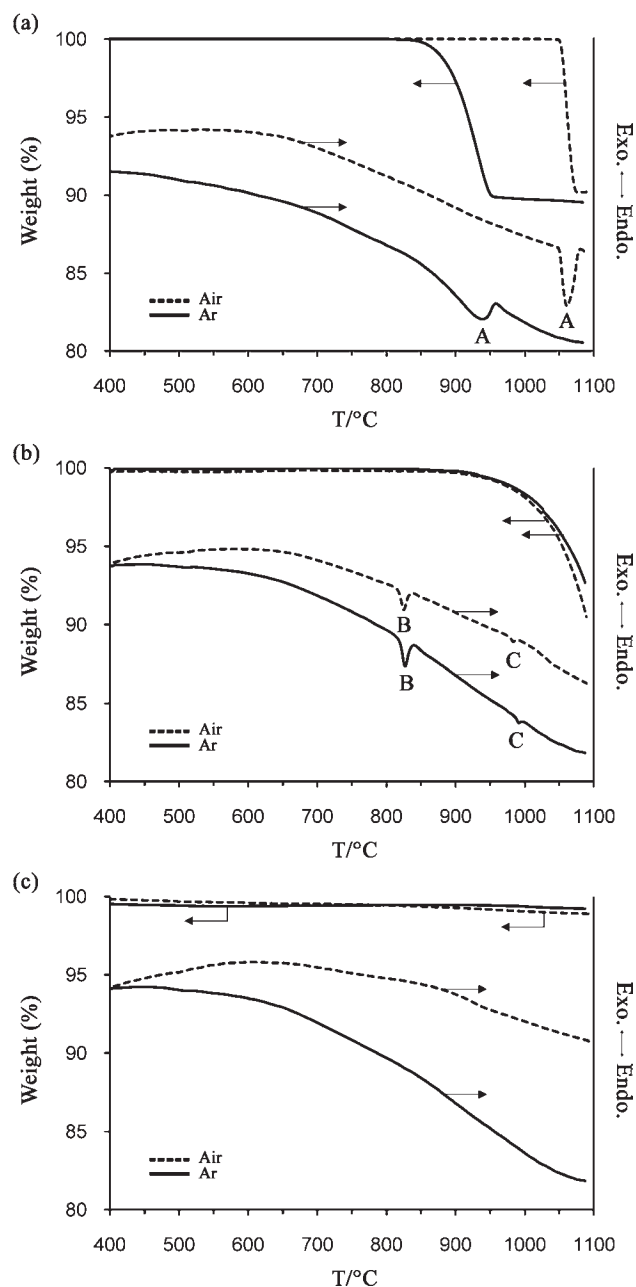
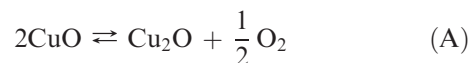


**Figure 3.** TGA-DTA spectra heated at  $10\text{ °C min}^{-1}$  in air and Ar for (a) CuO, (b) BaCO<sub>3</sub>, and (c) Y<sub>2</sub>O<sub>3</sub>.

We restrict our study to the reactions between Y<sub>2</sub>O<sub>3</sub>, BaCO<sub>3</sub>, and CuO. Since it is generally accepted that solid state reactions are sensitive to the atmosphere in which they occur, and more specifically to O<sub>2</sub> partial pressures, all TGA-DTA measurements were done both in air and Ar.<sup>26,27</sup>

**Separate Metal-Oxides and YBCO.** Figure 3a shows the TGA-DTA spectra obtained for CuO powder in air and Ar respectively. In both cases a mass drop of ~10% is found which can be correlated to the reduction of CuO to Cu<sub>2</sub>O. DTA analysis reveals that the reduction reaction is endothermic in both atmospheres. Since oxygen is

released during reduction, this reaction is atmosphere dependent.



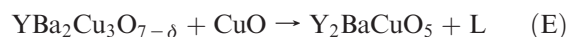
The maximum of the DTA-peak shifts from 1060 °C in air to 940 °C in Ar.

Figure 3b represents data from thermal analysis for BaCO<sub>3</sub> powder in air and Ar respectively. Both TGA spectra show that BaCO<sub>3</sub> is stable until 900 °C, and decarboxylation to BaO takes place over a broad temperature range. Even at 1100 °C, no complete combustion of the precursor is observed (mass loss < 22.3%). During combustion, no substantial DTA-deviation is observed. DTA-analysis shows two small endothermic peaks at 821 °C (B) and 989 °C (C), corresponding to crystallographic phase transitions of BaCO<sub>3</sub><sup>28</sup> from  $\gamma$ -orthorhombic (natural witherite) to  $\alpha$ -cubic over  $\beta$ -hexagonal.



Figure 3c represents the TGA-DTA spectra of Y<sub>2</sub>O<sub>3</sub> in air and Ar. Both TGA and DTA analysis show that Y<sub>2</sub>O<sub>3</sub> is stable until 1100 °C.

Figures 4a and 4b show the TGA-DTA spectra of YBCO during heating and cooling, respectively. The DTA-heating curves show a first exothermic reaction E at 960 °C in air and at 880 °C in Ar, which can be assigned according to the literature to the following peritectic transformation:<sup>29–31</sup>



The detection of a small amount of CuO in the melt-grown YBCO sample using XRD endorses this assumption. Further heating gives rise to two reversible reactions F and G respectively at 1040 and 1065 °C in air, 970 and 990 °C in Ar. Both reactions are accompanied by a small weight loss. The presence of exothermic peaks during cooling both in air and Ar suggests that these reactions are solidification reactions. Furthermore, only the sample heated in air shows a weight increase during cooling. This suggests that these reactions involve a change in oxygen stoichiometry.

**Binary Precursor Interactions.** Figure 5a represents the TGA-DTA spectra of a binary powder mixture of Y<sub>2</sub>O<sub>3</sub> and BaCO<sub>3</sub>. The two compounds were mixed in a Y/Ba-ratio of 1:2. No evidence of any chemical reaction between Y<sub>2</sub>O<sub>3</sub> and BaCO<sub>3</sub> is found.<sup>32</sup> Only the DTA peak (820 °C) related to the BaCO<sub>3</sub> crystal transition (B) is present. Because of the limited resolution of the experiment, the  $\beta$ - $\alpha$  transition (C) is not visible here.

(26) Feenstra, R.; Lindemer, T. B.; Budai, J. D.; Galloway, M. D. *J. Appl. Phys.* **1991**, *69*, 6569.

(27) Morris, D. E.; Markelz, A. G.; Fayn, B.; Nickel, J. H. *Phys. Chem. (Amsterdam, Neth.)* **1990**, *168*, 153.

(28) Pasierb, P.; Gajerski, R.; Rokita, M.; Rekas, M. *Phys. B (Amsterdam, Neth.)* **2001**, *304*, 463.

(29) Gervais, M.; Odier, P.; Coutures, J. P. *Mater. Sci. Eng., B* **1991**, *8*, 287.

(30) Kosmynin, A. S.; Shter, G. E.; Garkushin, I. K.; Trunin, A. S.; Balashov, V. A.; Fotiev, A. A. *Supercond.: Phys. Chem. Technol.* **1990**, *3*, S271.

(31) Krabbes, G.; Bieger, W.; Wiesner, U.; Ritschel, M.; Teresiak, A. *J. Solid State Chem.* **1993**, *103*, 420.

(32) Zhang, W.; Osamura, K. *Mater. Trans., JIM* **1991**, *32*, 1048.

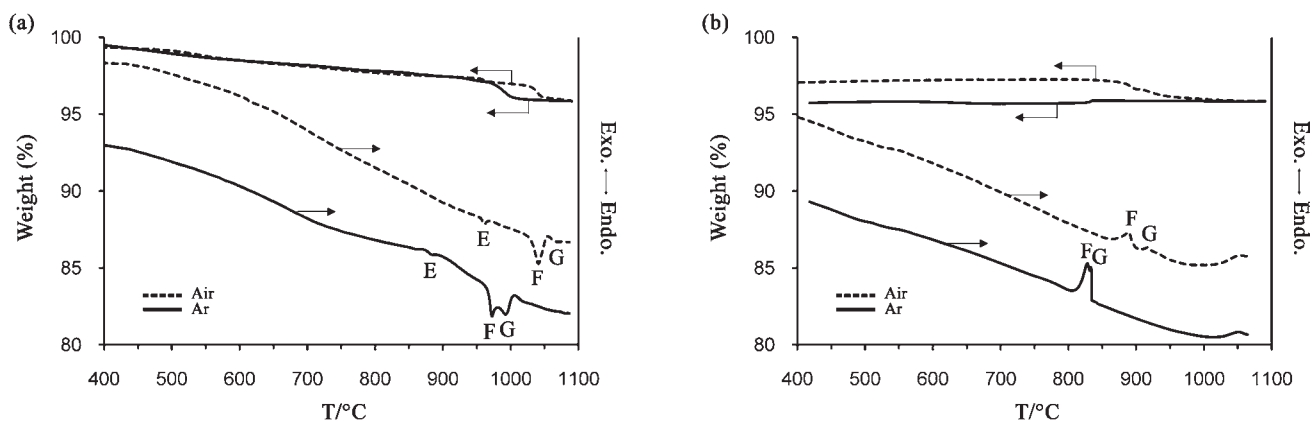


**Figure 4.** TGA-DTA spectra of  $\text{YBa}_2\text{Cu}_3\text{O}_{7-\delta}$  in air and Ar using (a) a heating ramp of  $10\text{ }^\circ\text{C min}^{-1}$  and (b) a cooling ramp of  $20\text{ }^\circ\text{C min}^{-1}$ .

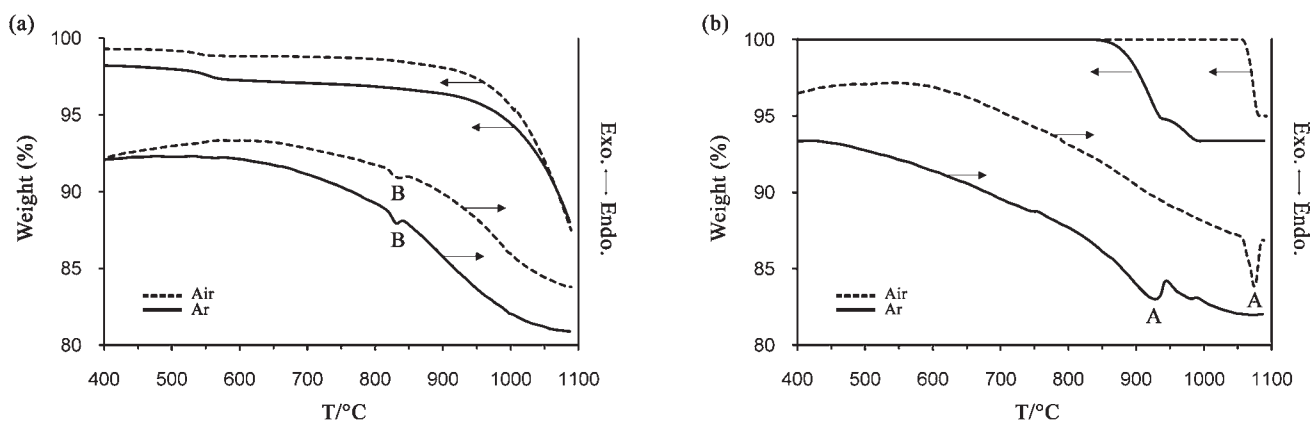


**Figure 5.** TGA-DTA spectra in air and Ar for binary mixtures of (a)  $\text{Y}_2\text{O}_3:\text{BaCO}_3$  (Y/Ba = 1:2) and (b)  $\text{Y}_2\text{O}_3:\text{CuO}$  (Y/Cu = 1:3) both heated at  $10\text{ }^\circ\text{C min}^{-1}$ .

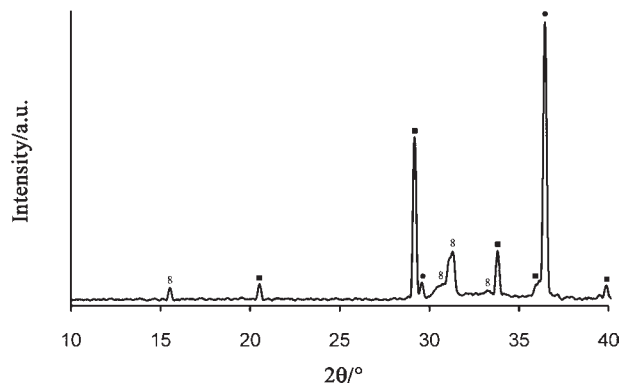


**Figure 6.** XRD spectrum of an  $\text{Y}_2\text{O}_3:\text{CuO}$  (Y/Cu = 1:3) mixture heated at  $1000\text{ }^\circ\text{C}$  for 24 h in  $\text{N}_2$  (■)  $\text{Y}_2\text{O}_3$ , (●)  $\text{Cu}_2\text{O}$  and (8) yttriumcuprate.

Figure 5b shows the TGA-DTA spectra of the binary mixture of  $\text{Y}_2\text{O}_3$  and  $\text{CuO}$ . The two compounds were mixed in a Y/Cu-ratio of 1:3. As for pure  $\text{CuO}$ , two endothermic peaks are found at  $1060$  and  $940\text{ }^\circ\text{C}$ , respectively. TGA analysis in Ar shows an extra mass drop of  $1.5\%$  which is associated with a slightly endothermic deviation in the DTA-curve. XRD analysis (Figure 6) of the final product identified the existence of an yttriumcuprate.

Finally, Figure 7a represents the TGA-DTA spectra of the binary mixture of  $\text{BaCO}_3$  and  $\text{CuO}$ . The two compounds were mixed in a Ba/Cu-ratio of 2:3.

Under air, a first decrease in mass is detected at  $700\text{ }^\circ\text{C}$ , while for pure  $\text{CuO}$  (Figure 3a) and  $\text{BaCO}_3$  (Figure 3b),

the first mass losses start to appear at higher temperatures,  $1050$  and  $900\text{ }^\circ\text{C}$  respectively. This suggests that a reaction between  $\text{BaCO}_3$  and  $\text{CuO}$  takes place.

At  $990\text{ }^\circ\text{C}$ , a final mass loss of  $15.2\%$  is observed while for a separated decarboxylation and reduction a theoretical mass loss of  $17.7\%$  is expected.

From the literature it is established that if  $\text{BaCO}_3$  and  $\text{CuO}$  are mixed in a Ba/Cu 1:1 ratio, (i)  $\text{CuO}$  can act as a catalyst in the decarboxylation of  $\text{BaCO}_3$  and (ii) decarboxylation of  $\text{BaCO}_3$  proceeds simultaneously with the formation of  $\text{BaCuO}_2$ .<sup>33</sup> XRD analysis (Figure 8) confirms the formation of  $\text{BaCuO}_2$ , which is in agreement with the  $\text{BaCO}_3(\text{BaO})\text{-CuO}$  phase diagrams in the literature.<sup>34–36</sup>



In our case, excess  $\text{CuO}$  is present in the mixture so that  $\text{BaCuO}_2$  can further react with the remaining  $\text{CuO}$  forming a eutectic liquid.<sup>37</sup>



Since reaction H is quite slow,<sup>33</sup> a low heating rate of  $1\text{ }^\circ\text{C min}^{-1}$  was used in the TGA-DTA experiment to improve conversion of reaction H, before reaction I starts.

(33) Itoh, T. *J. Mater. Sci. Lett.* **2003**, *22*, 185.

(34) Voronin, G. F.; Degterov, S. A. *J. Solid State Chem.* **1994**, *110*, 50.

(35) Wong-Ng, W.; Cook, L. P. *J. Am. Ceram. Soc.* **1994**, *77*, 1883.

(36) Zhang, W.; Osamura, K.; Ochiai, S. *J. Am. Ceram. Soc.* **1990**, *73*, 1958.

(37) Chu, P. Y.; Buchanan, R. C. *J. Mater. Res.* **1993**, *8*, 2134.

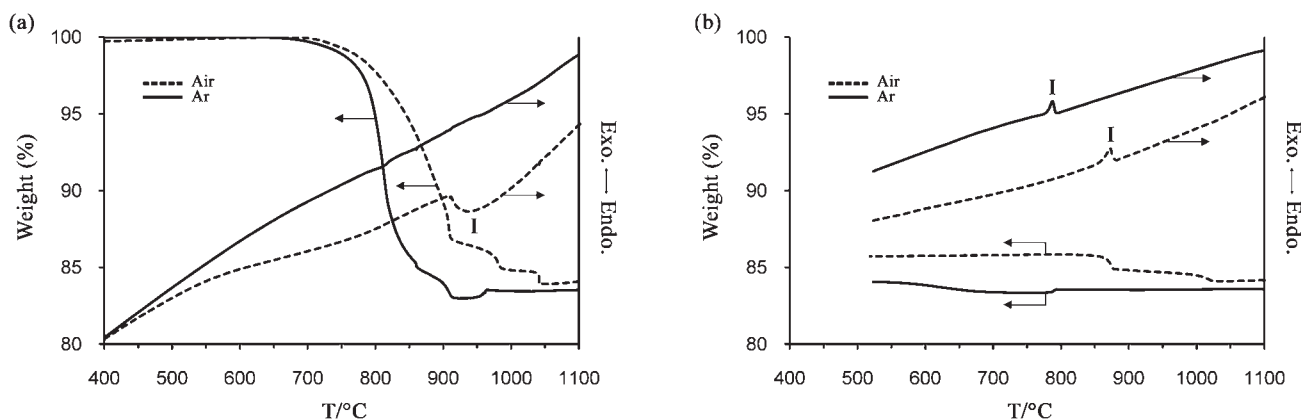


**Figure 7.** TGA-DTA spectra of a binary mixture of BaCO<sub>3</sub> and CuO (Ba/Cu = 2:3) in air and Ar when (a) heated at 1 °C min<sup>-1</sup> and (b) cooled at 20 °C min<sup>-1</sup>.

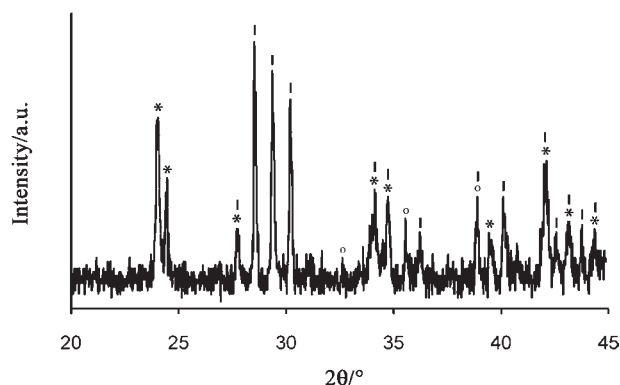


**Figure 8.** XRD spectrum of a BaCO<sub>3</sub>:CuO mixture heated at 1000 °C for 1 h in N<sub>2</sub>, (\*) BaCO<sub>3</sub>, (o) CuO, and (|) BaCuO<sub>2</sub>.

The first mass drop of 13.2% in the TGA-DTA spectrum corresponds with the formation of BaCuO<sub>2</sub> according to reaction H (13.9%). The small deviation in mass loss can be associated to an incomplete reaction. Second, BaCuO<sub>2</sub> reacts eutectically with CuO in accordance with reaction I. A gradual exponential mass loss in combination with an endothermic DTA signal during heating and a microscopic image showing a typical pattern of solidification after cooling (Figure 9) endorse this assumption. Furthermore, this is in good agreement with the published phase diagrams.<sup>34–36</sup>

A third mass loss can be correlated to a deviation in oxygen content. During cooling (Figure 7b) an equivalent amount of oxygen is absorbed. Furthermore, the DTA analysis during cooling shows an exothermic deviation, which can be associated with the solidification of the liquid. Therefore, the exothermic peak in Figure 7b is associated with the backward reaction of I and forms an extra endorsement of the existence of reaction I.

Under Ar, a similar pattern is obtained. Here, the first mass drop is 14.5% instead of 13.2%. This difference corresponds to the reduction of the remaining CuO. In air, this reduction does not take place because temperatures of 1050 °C and more are necessary to induce reduction. Yet, at 980 °C all CuO present is already consumed in reactions H and I.

The presence of a mass increase under Ar around 950 °C is probably an anomaly because of an incomplete adaptation of the furnace atmosphere.

When the TGA-DTA spectra are recorded using a heating ramp of 10 °C min<sup>-1</sup> instead of 1 °C min<sup>-1</sup> (Figure 10), the formation of BaCuO<sub>2</sub> is still incomplete before CuO starts to reduce and liquid formation starts. For this reason, BaCO<sub>3</sub> phase transition (B) and CuO reduction (A) are visible in the DTA-curves. As all reactions take place simultaneously, only the characteristic peaks A and B are assigned.

The above results for binary precursor interactions suggest that the reaction between BaCO<sub>3</sub> and CuO has a predominant role in the formation of YBCO starting from non-fluorine precursors. To verify this, ternary precursor interactions were studied.

**Ternary Precursor Interactions.** The TGA-DTA spectra for a powder mixture of Y<sub>2</sub>O<sub>3</sub>, BaCO<sub>3</sub>, and CuO in a Y/Ba/Cu-ratio of 1:2:3 are shown in Figure 11. This ternary mixture starts to lose weight from 800 °C. In Ar, the mass loss until 910 °C can be associated to the simultaneous reactions involving (i) decarboxylation of BaCO<sub>3</sub>, (ii) reduction of CuO, and (iii) formation of BaCuO<sub>2</sub>. The theoretical mass loss of 12.9% matches the experimental mass loss of 13%. This is in agreement with the observations obtained for the binary BaCO<sub>3</sub>:CuO mixture. At 920 °C a small mass loss is observed in TGA, probably resulting from the eutectic reaction between BaCuO<sub>2</sub> and CuO. Subsequently, at 935 °C, an exothermic reaction J takes place: Y<sub>2</sub>O<sub>3</sub> reacts most likely with the eutectic liquid obtained in reaction I to form YBa<sub>2</sub>Cu<sub>3</sub>O<sub>6+x</sub>.



At 970 and 990 °C, the characteristic endothermic peaks F and G correlate to the decomposition of YBCO. The temperatures are similar to the decomposition temperatures of pure YBCO-powder (Figure 4a). In air a similar pattern is observed.

**Part B: Thin Films.** Since coated conductors are composed of thin YBa<sub>2</sub>Cu<sub>3</sub>O<sub>7-δ</sub> films, it was verified if the YBCO reaction mechanism presented here is also valid in the case of thin films prepared from an aqueous fluorine-free sol-gel precursor. Therefore a HT-XRD experiment was performed. A first experiment was set up to examine the reaction behavior in BaCO<sub>3</sub>-CuO films. Therefore, a sol-gel precursor containing Ba- and Cu-acetate in a Ba/Cu ratio of 2:3 was dip-coated



**Figure 9.** Microscopic image of the  $\text{BaCO}_3\text{-CuO}$  powder after TGA-DTA analysis.

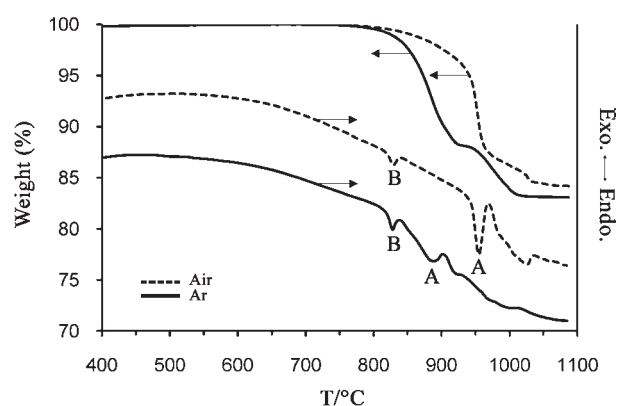


**Figure 10.** TGA-DTA spectra of a binary mixture of  $\text{BaCO}_3\text{:CuO}$  ( $\text{Ba/Cu} = 2:3$ ) in air and Ar when heated at  $10^\circ\text{C min}^{-1}$ .

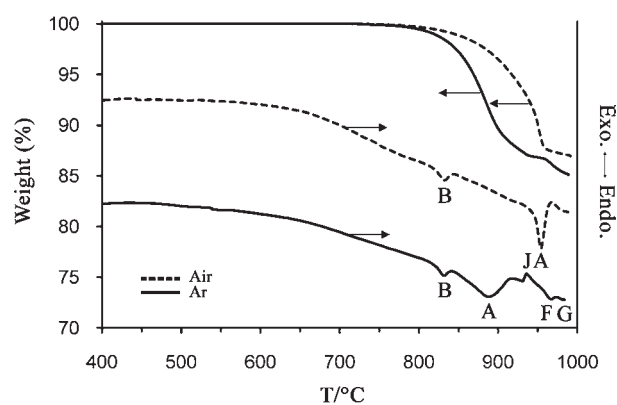
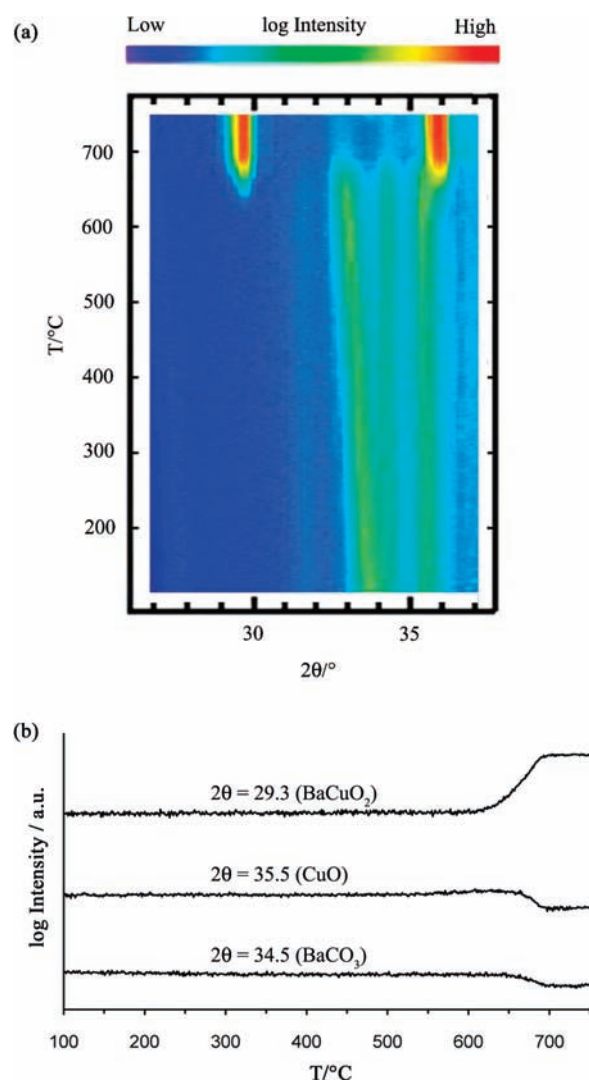


**Figure 11.** TGA-DTA spectra of a ternary mixture of  $\text{Y}_2\text{O}_3$ ,  $\text{BaCO}_3$ , and  $\text{CuO}$  ( $\text{Y/Ba/Cu} = 1:2:3$ ) in air and Ar when heated at  $10^\circ\text{C min}^{-1}$ .

on a STO substrate. The film was burned out at  $500^\circ\text{C}$  resulting in a film containing  $\text{BaCO}_3$  and  $\text{CuO}$ . This temperature was chosen based on the TGA-DTA spectrum of the separated acetates (Figure 1).

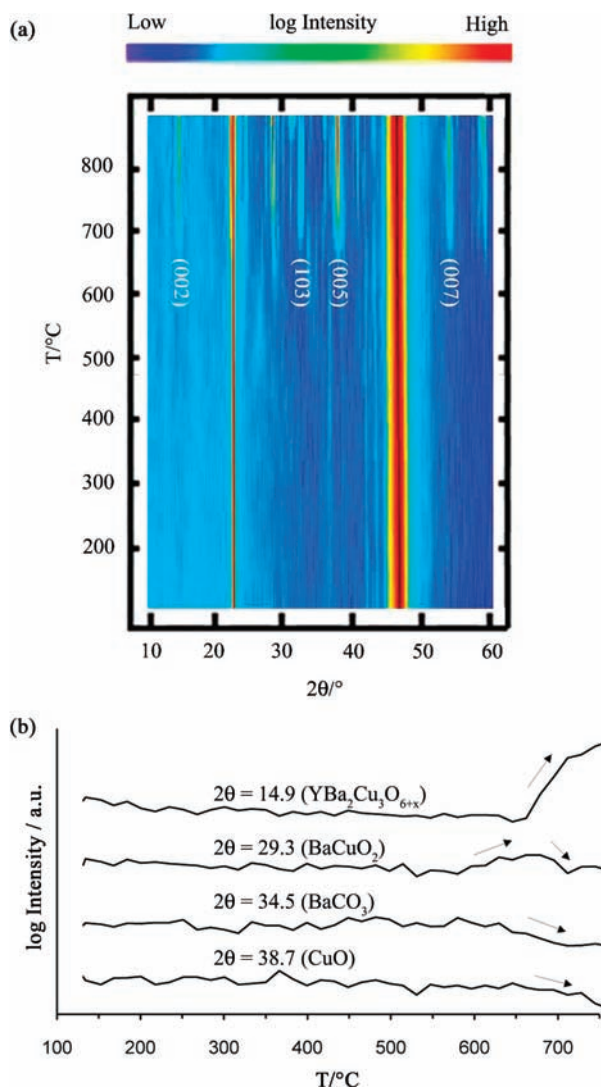
Subsequently, the film was placed in the furnace of the HT-XRD and heated at  $10^\circ\text{C min}^{-1}$  until  $750^\circ\text{C}$  under a flowing He atmosphere.

Figure 12 shows the HT-XRD measurement of a  $\text{BaCO}_3\text{-CuO}$  thin film. Up to  $640^\circ\text{C}$ ,  $\text{BaCO}_3$  ( $2\theta = 33.7^\circ$ ,



**Figure 12.** HT-XRD measurement of a  $\text{BaCO}_3\text{-CuO}$  film under He with a heating ramp of  $10^\circ\text{C min}^{-1}$  (a) full  $2\theta$ -scan plot (b) log intensity plot of important compounds.

$34.5^\circ$ ) and  $\text{CuO}$  ( $2\theta = 35.5^\circ$ ) are present in the layer. At  $640^\circ\text{C}$   $\text{BaCO}_3$  decomposes and  $\text{BaCuO}_2$  ( $2\theta = 29.3^\circ$ ) is formed. At that time,  $\text{CuO}$  reduces to  $\text{Cu}_2\text{O}$  ( $2\theta = 36.5^\circ$ ).



**Figure 13.** HT-XRD measurement of a  $\text{Y}_2\text{O}_3$ - $\text{BaCO}_3$ - $\text{CuO}$  film under a 200 ppm  $\text{O}_2$ : $\text{N}_2$  atmosphere with a heating ramp of  $10\text{ }^\circ\text{C min}^{-1}$  (a) full  $2\theta$ -scan plot and (b) log intensity plot of important compounds.

Small deviations from theoretical  $2\theta$ -values at higher temperatures are the result of thermal expansion of the material. The decomposition temperature of  $\text{BaCO}_3$  is much lower in thin films ( $640\text{ }^\circ\text{C}$ ) than in powders because the grain size is much smaller for the particles in the precursor solution than those obtained from powder mixing.<sup>37</sup>

Second, a ternary  $\text{Y}_2\text{O}_3$ - $\text{BaCO}_3$ - $\text{CuO}$  film was examined with HT-XRD. Therefore, a sol-gel precursor containing Y-, Ba-, and Cu-acetate in a Y/Ba/Cu ratio of 1:2:3 was dip-coated on a STO substrate. Again, the film was burned out at  $500\text{ }^\circ\text{C}$  resulting in a film containing  $\text{Y}_2\text{O}_3$ ,  $\text{BaCO}_3$ , and  $\text{CuO}$ . Subsequently, the film was placed in the HT-XRD where it was heated until  $900\text{ }^\circ\text{C}$  at a heating rate of  $10\text{ }^\circ\text{C min}^{-1}$ . The ruling atmosphere was a flowing 200 ppm  $\text{O}_2$ : $\text{N}_2$  mixture. This atmosphere

was already successfully used in previous research to prepare superconducting YBCO films on STO substrates with the same precursor solution.<sup>24</sup>

Figure 13a shows the HT-XRD measurement of a  $\text{Y}_2\text{O}_3$ - $\text{BaCO}_3$ - $\text{CuO}$  thin film. Strong (00 L) STO reflections are present at  $2\theta$  values of  $22.8^\circ$  and  $46.5^\circ$ .

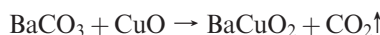
$\text{BaCO}_3$  ( $2\theta = 34.5^\circ$ ) and  $\text{CuO}$  ( $2\theta = 35.5^\circ$  and  $38.7^\circ$ ) reflections started to disappear around  $650\text{ }^\circ\text{C}$ , with the formation of  $\text{BaCuO}_2$  ( $2\theta = 29.3^\circ$ ) as a result. Subsequently, the formation of preferentially  $c$ -axis oriented YBCO started ( $2\theta = 14.9^\circ$ ,  $37.9^\circ$  and  $54.2^\circ$ ).

This HT-XRD experiment confirms the results obtained for bulk materials: (i) the formation mechanism of non-fluorine prepared YBCO is dominated by the Ba-Cu interactions, and (ii)  $\text{BaCuO}_2$  is an intermediate in the formation mechanism of YBCO.

## Conclusions

Within this study, the objective was to investigate (i) the YBCO reaction mechanism for fluorine-free approaches and (ii) the role of  $\text{BaCO}_3$  in the production of superconducting materials. First, an intensive TGA-DTA study on bulk materials suggests a three step mechanism for the formation of YBCO.

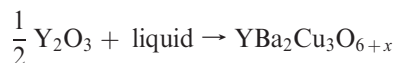
In a first step  $\text{BaCO}_3$  and  $\text{CuO}$  react to form  $\text{BaCuO}_2$ :



In a next step, which can be simultaneous with the previous step, the intermediate  $\text{BaCuO}_2$  will react with  $\text{CuO}$  to form a liquid:



Finally, the liquid will react with  $\text{Y}_2\text{O}_3$  to form YBCO:



Within this mechanism,  $\text{BaCO}_3$  has clearly a predominant role.

HT-XRD experiments confirmed that the results obtained for bulk mixtures are also applicable in the case of thin films. This mechanism explains the presence and consumption of  $\text{BaCO}_3$  during thin film synthesis starting from non-fluorine precursors.

This study establishes clearly that the presence of  $\text{BaCO}_3$  is not fatal in obtaining an YBCO compound. Moreover, this paper gives a suitable explanation to the fact why  $\text{BaCO}_3$  was a desired intermediate phase in the production of YBCO thin films starting from an aqueous non-fluorine precursor, as published before.<sup>24</sup>

**Acknowledgment.** Bart Ruttens is gratefully acknowledged for performing HT-XRD measurements. K.V. is a postdoctoral fellow with the Fund for Scientific Research-Flanders (Belgium) (FWO Vlaanderen).